Effect of the Smear and Transition Zones around Prefabricated Vertical Drains Installed in a Triangular Pattern on the Rate of Soil Consolidation

D. Basu, S.M.ASCE[1]; and M. Prezzi, M.ASCE[2]

Abstract: Soil disturbance caused by the installation of prefabricated vertical drains (PVDs) has a large impact on the rate of consolidation. It is essential in design to quantify this effect. In this paper, we investigate the consolidation rate of soils with PVDs installed in a triangular pattern using two-dimensional finite-element analysis with full consideration of disturbance effects. This is done by accounting for the transition zone that exists between the highly disturbed smear zone and the undisturbed zone. The hydraulic conductivity in the transition zone is assumed to increase linearly from a low value in the smear zone to the original in situ value in the undisturbed zone. The actual band shape of the PVD and hexagonal zone of influence around it are used in the analysis. In addition to soil disturbance effects, the influence on consolidation rate of the size of the smear and the transition zones, the PVD spacing, and the mandrel size and shape is also investigated. Guidelines are given for using an equivalent system, where the transition zone is replaced by an expanded smear zone producing the same effect. This equivalent-system approach allows use of existing analytical solutions that consider only the smear zone in analysis and design.

DOI: 10.1061/(ASCE)1532-3641(2007)7:1(34)

CE Database subject headings: Drains; Soil consolidation; Ground stabilization; Finite element method.

Introduction

Thick deposits of soft, saturated clays have low shear strength, high compressibility, and low hydraulic conductivity. Consequently, there is often the need to use techniques such as preloading to increase their strength and stiffness. Preloading is often combined with the installation of vertical drains to speed up the consolidation process and hence increase the strength gain rate (Holtz 1987; Bergado et al. 1993a). Currently, band-shaped prefabricated vertical drains (PVDs) are frequently used in practice. The PVDs are installed at regular intervals in a square, rectangular, or triangular pattern (Bergado et al. 1996), with center to center distance varying from about 1.0 to 3.5 m (Holtz 1987). A typical PVD cross section consists of a plastic core which is wrapped around by a filter sleeve, and has dimensions of 100 mm $\times$ 4 mm (Holtz 1987). The excess pore pressure generated due to preloading quickly dissipates due to the easy outflow of water through the PVD.

Notwithstanding the successful use of PVDs, there are certain operational problems associated with them (Akagi 1994; Holtz 1987). PVDs are installed using closed-ended mandrels. The installation of the PVDs significantly disturbs the surrounding soil. There is an increase in pore pressure, decrease in strength and water content in the disturbed soil (Holtz and Holm 1973). Also, the hydraulic conductivity of the disturbed soil is reduced below its initial value before the PVD installation (Holtz and Holm 1973). Consequently, the flow of water into the PVD is slowed down and the consolidation process is significantly delayed.

The disturbed zone around the PVD consists of basically two zones: the smear zone and the transition zone (Bergado et al. 1996; Madhav et al. 1993). The smear zone is the completely remolded zone of soil immediately adjacent to the drain. The transition zone, which separates the smear zone from the undisturbed zone (Onoue et al. 1991; Madhav et al. 1993; Indraratna and Redana 1998; Sharma and Xiao 2000), is the zone in which there is a gradual transition of soil properties, with the degree of disturbance decreasing with increasing distance from the drain (Holtz and Holm 1973).

Many researchers have investigated the size of the smear zone and the degree of disturbance in it. Studies by Holtz and Holm (1973), Jamiolkowski et al. (1983), Hansbo (1986, 1987, 1997), Bergado et al. (1991, 1993b), Onoue et al. (1991), Holtz et al. (1991), Mesri et al. (1994), Madhav et al. (1993), and Chai and Miura (1999) suggest that the size of the smear zone (i.e., the distance from the center of a drain to the outer boundary of the smear zone) varies between 1 and 4 times the equivalent mandrel radius $r_{m,\mathrm{eq}}$ (the mandrel cross section, if not circular in shape, is converted to an equivalent circle with radius $r_{m,\mathrm{eq}}$ that has the same area as that of the actual mandrel cross section). Other studies (by Hansbo 1987; Chai and Miura 1999; Hird and Moseley 2000) suggested that the size of the smear zone is in a range from 2 to 3 times $r_{m,\mathrm{eq}}$. These values are based mostly on field investigations, back calculations from case histories, theoretical considerations, and experience (Hird and Moseley 2000). It is important to note that the values proposed by some of the researchers

[1]Doctoral Candidate, School of Civil Engineering, Purdue Univ., 550 Stadium Mall Dr., West Lafayette, IN 47907. E-mail: dbasu@purdue.edu

[2]Assistant Professor, School of Civil Engineering, Purdue Univ., 550 Stadium Mall Dr., West Lafayette, IN 47907. E-mail: mprezzi@purdue.edu

Note. Discussion open until July 1, 2007. Separate discussions must be submitted for individual papers. To extend the closing date by one month, a written request must be filed with the ASCE Managing Editor. The manuscript for this paper was submitted for review and possible publication on May 18, 2005; approved on December 16, 2005. This paper is part of the ***International Journal of Geomechanics***, Vol. 7, No. 1, February 1, 2007. ©ASCE, ISSN 1532-3641/2007/1-34–43/$25.00.

(Jamiolkowski et al. 1983; Bergado et al. 1991, 1993b) already incorporate the effect of the transition zone.

The degree of disturbance can be expressed in terms of the ratio k_{hs}/k_{ho} of the horizontal hydraulic conductivity of the smear zone to that of the undisturbed zone. Bergado et al. (1993a,b), Hansbo (1986, 1997), Madhav et al. (1993), and Hird and Moseley (2000) found, based on field data, laboratory tests, model studies, and practical considerations, that k_{hs}/k_{ho} varies between 0.1 and 0.33. Casagrande and Poulos (1969) suggested a lower value (0.001) for k_{hs}/k_{ho} based on analyses of case histories, whereas Bergado et al. (1991) and Onoue et al. (1991) suggested higher values (0.5–0.66) based on laboratory tests.

The existence of the transition zone was experimentally confirmed by Onoue et al. (1991). They found that the outer boundary of the transition zone, measured from the center of the drain, lies at a distance of about 6 to 7 times the equivalent mandrel radius, and the hydraulic conductivity within the transition zone increases approximately linearly (from k_{hs} to k_{ho}) as the distance from the drain increases. The approximate linear variation of hydraulic conductivity was also observed in the laboratory experiments by Indraratna and Redana (1998) and Sharma and Xiao (2000). The outer boundary of the transition zone, measured from the center of the drain, extended to a distance of more than 7 times the equivalent mandrel radius in the experiments of Indraratna and Redana (1998), whereas, in the experiments by Sharma and Xiao (2000), it extended to about 10–15 times the equivalent mandrel radius. Madhav et al. (1993) performed laboratory tests on samples collected from a site where PVDs had been installed with a square mandrel and found that the width of the transition zone (twice the distance from the center of the drain to the outer boundary of the mandrel) is about 12 times the width of the mandrel. They further observed that, within the transition zone, the average hydraulic conductivity values had an approximate linear relationship with distance from the center of the drain, even if large scatter was observed. A similar, approximately linear variation was assumed by Miura et al. (1993) as well. Based on studies on pile driving in clay, Jamiolkowski et al. (1983) suggested that the transition zone diameter can be as large as 20 times the equivalent mandrel diameter.

Most analyses of vertical drains, accounting for soil disturbance, consider only the smear zone. Barron (1948) developed closed-form solutions for the rate of consolidation considering only radial flow with and without a smear zone around the drain. A simplified analytical solution was later obtained by Hansbo (1981) for PVDs with a smear zone. The solutions of Barron (1948) and Hansbo (1981) assume a circular drain and a circular zone of influence around the drain. Leo (2004) developed an analytical solution by considering vertical flow in addition to radial flow. He observed that the vertical flow has a negligible contribution to the consolidation rate. Analyses using finite difference and finite-element methods accounting for the smear zone have also been performed (Madhav et al. 1993; Bergado et al. 1993b; Basu and Madhav 2000; Indraratna and Redana 1997). The transition zone has been taken into account in a limited number of studies, which include the numerical studies of Madhav et al. (1993) and Hawlader et al. (2002) and an analytical solution by Chai et al. (1997).

In this paper, we investigate the consolidation rate of soils with PVDs using two-dimensional finite-element (FE) analysis with full consideration of disturbance effects. The Terzaghi-Rendulic theory of consolidation (Terzaghi 1925; Rendulic 1935, 1936) is used. In order to study the effect of soil disturbance on PVD performance, both the smear and transition zones are considered

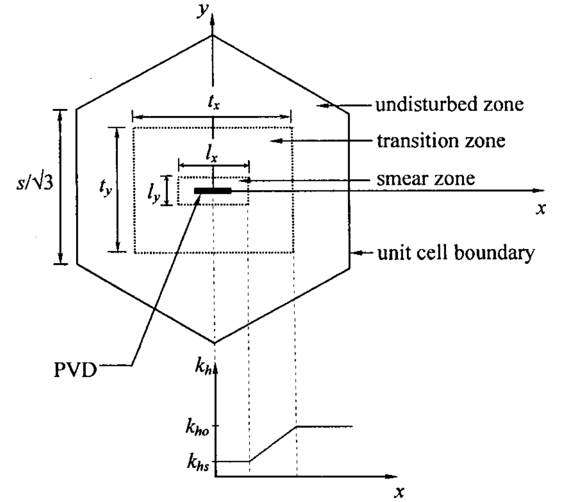

Fig. 1. Hexagonal unit cell with rectangular disturbed zone

in the analysis. It is assumed that PVDs with cross-section dimensions of 100 mm $\times$ 4 mm are installed in a triangular pattern with a center-to-center spacing equal to s. The resulting area of influence of a PVD (hereafter referred to as "unit cell") is a regular hexagon with the length of each side equal to $s/\sqrt{3}$ (Fig. 1). The smear and transition zones surrounding the PVD are assumed to have rectangular shape. The actual hexagonal shape of the unit cell, the band shape of the PVD, and the rectangular shape of the smear and transition zones are used in the analysis. A method of replacing the transition zone by an equivalent expanded smear zone is outlined so that existing analytical solutions considering only a smear zone can be used in design.

Characterization of Disturbed Zone

Smear and Transition Zones

Since the mandrel displaces and drags down the surrounding soil during PVD installation, the shape and size of the smear and transition zones in plan depend primarily on the shape and size of the mandrel cross section. Accordingly, the values for the size of the smear and transition zones proposed in the literature are mostly related to the mandrel size. However, other factors like mandrel driving speed, mandrel end shoe, and soil properties also affect the size of the disturbed zone (Holtz et al. 1991; Hird and Moseley 2000). Since the values proposed in the literature are mostly based on field studies and analysis of case histories, they incorporate the effects of all these factors. In this paper, the smear and transition zone dimensions are chosen based on the values proposed in the literature.

Four rectangular mandrels (125×50, 150×50, 120×120, and 150×150, all in millimeters) are considered (Bergado et al. 1993b; Madhav et al. 1993; Saye 2003; American Wick Drain Corporation 2004). The mandrels with rectangular cross section are likely to create smear and transition zones that have rectangular or nearly rectangular (e.g., elliptical) shape in plan (Chai and Miura 1999). In this analysis, the smear and transition zones are assumed to be rectangular with dimensions $l_x \times l_y$ and $t_x \times t_y$, respectively (Figs. 1 and 2).

When a rectangular mandrel is pushed into soil, the conditions along the larger side of the mandrel (where the soil was displaced by a value equal to the width d of the mandrel) are quite uniform,

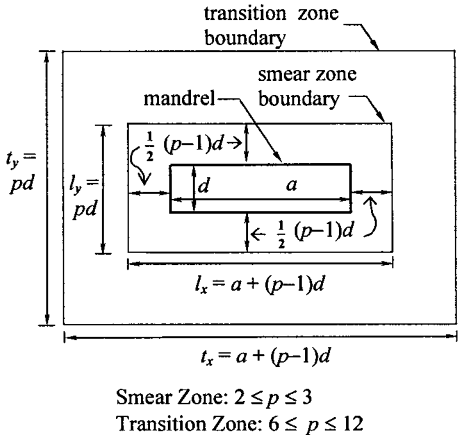

Fig. 2. Smear and transition zone dimensions in terms of mandrel size

with deviations in the state of strain around the mandrel appearing only near the corners with the smaller side. Accordingly, the size of the smear zone must depend to a large extent on the smaller dimension (the width d of the mandrel) of the rectangular mandrel and not on its equivalent diameter $d_{m,\text{eq}}$. Assuming that the thickness of the smear zone surrounding the mandrel remains constant along the entire mandrel perimeter (Fig. 2), the dimensions $l_x \times l_y$ of the smear zone can be obtained from

$$l_y = pd \tag{1}$$

$$l_x = a + (p-1)d \tag{2}$$

where p=parameter such that $2 \leqslant p \leqslant 3$ and a and d=dimensions of the mandrel cross section with $a > d$. The transition zone dimensions $t_x \times t_y$ can likewise be obtained from Eqs. (1) and (2), where l_y and l_x are replaced by t_y and t_x, respectively, with p ranging between 6 and 12. The choice of p values for the smear and transition zones is consistent with the values found in the literature.

Since the mechanisms determining the shape and size of the disturbed zone are not fully understood, simulations were performed to confirm that the assumption of a rectangular disturbed zone was acceptable. The consolidation rate was studied by varying l_x for fixed values of l_y. It was observed that, for a given l_y, the rate of consolidation does not vary much with l_x. It is the thickness l_y and not the overall shape of the rectangle that controls the consolidation. Further, this suggests that as long as the thickness l_y remains more or less constant, the exact shape of the smear zone (whether it is rectangular or slightly elliptical) will not affect the consolidation rate to a large extent. This observation is consistent with the FE analysis of Chai and Miura (1999), according to which the difference in the consolidation rate due to the assumption of a circular smear zone and a rectangular smear zone with the same area is negligible.

Hydraulic Conductivity

The hydraulic conductivity in the smear and the undisturbed zones are assumed to be constants with values k_{hs} and k_{ho}, respectively, whereas it increases linearly in the transition zone from k_{hs} to k_{ho} as the distance from the PVD surface increases (Fig. 1). At any distance within the transition zone, the hydraulic conductivity in the x direction is given by

$$k_{ht}(x) = k_{hs} + \frac{2x - l_x}{t_x - l_x}(k_{ho} - k_{hs}) \quad (l_x/2 \leqslant x \leqslant t_x/2) \tag{3}$$

A similar expression for the variation of k_{ht} in the y direction can be obtained by replacing y for x, l_y for l_x, and t_y for t_x.

Analysis

Consolidation is a time-dependent process that is generally expressed in terms of the time factor T, which is time normalized with respect to the dimensions of the soil volume to be drained and its coefficient of consolidation

$$T = \frac{c_h t}{d_{c,\text{eq}}^2} \tag{4}$$

where $d_{c,\text{eq}}$=diameter of a circle with the same area as the unit cell; it is a representative drainage path length. $d_{c,\text{eq}}$ for the case of a hexagonal domain is given by

$$d_{c,\text{eq}} = \sqrt{\frac{2\sqrt{3}}{\pi}}s \tag{5}$$

The degree of consolidation U at any particular time (or time factor) is the ratio of the average excess pore-water pressure already dissipated to its initial value. Mathematically, for two-dimensional consolidation, U can be expressed in terms of integrals of the pore-pressure over the unit cell domain as (Madhav et al. 1993)

$$U = 1 - \frac{\int_y \int_x u(x,y,T)dxdy}{\int_y \int_x u_{\text{ini}} dxdy} \tag{6}$$

where $u(x,y,T)$=excess pore pressure at any point with coordinates (x,y) at a time factor T, and u_{ini} is the initial excess pore pressure. The integrals in Eq. (6) are evaluated by a Gauss-quadrature integration scheme after obtaining the values of pore pressure u at the Gauss points within each element of the finite-element mesh (Cook et al. 2002).

The change in u with time (or time factor) over the entire domain needs to be known. This is described by the Terzaghi-Rendulic differential equation for two-dimensional consolidation as

$$\frac{\partial u}{\partial T} = d_{c,\text{eq}}^2 \left(\frac{\partial^2 u}{\partial x^2} + \frac{\partial^2 u}{\partial y^2} \right) \tag{7}$$

Eq. (7) is valid for a homogeneous and isotropic soil. However, when the soil is disturbed, the homogeneity of soil properties within the unit cell is lost. In such a situation Eq. (7) is modified as

$$\frac{\partial u}{\partial T} = d_{c,\text{eq}}^2 \frac{k_{hd}}{k_{ho}} \left(\frac{\partial^2 u}{\partial x^2} + \frac{\partial^2 u}{\partial y^2} \right) \tag{8}$$

where k_{hd}=hydraulic conductivity within any element lying in the disturbed zone. It is assumed that soil disturbance only affects the hydraulic conductivity and not the compressibility of the soil (Hansbo 1981; Madhav et al. 1993). If the element lies within the smear zone, then k_{hd} is equal to k_{hs}. On the other hand, if the element lies in the transition zone, then k_{hd} is equal to k_{ht}.

As a symmetric flow pattern exists with respect to the coordinate axes (Fig. 1), only the domain within the first quadrant (within which $x \geqslant 0$ and $y \geqslant 0$) is analyzed. The PVD thickness of 4 mm is neglected.

Initial and boundary conditions are needed for the solution of Eqs. (7) and (8). For the boundary that represents the interface between the PVD and soil (referred to as drain boundary hereafter), a value of $u=0$ is prescribed (Dirichlet boundary condition) because free flow occurs across it. For the remaining boundaries, the Neumann boundary condition $\partial u / \partial n = 0$ is prescribed because no flow is possible across them (n denotes the direction of the unit normal vector at the boundary surface).

The initial condition imposed is $u_{\text{ini}} = u(x, y, 0) = 100$ within the domain and at all the boundaries except at the drain boundary ($0 \leqslant x \leqslant 50$ mm, $y=0$), where the excess pore pressure dissipates instantaneously. Since drainage occurs immediately at the drain boundary, the initial condition prescribed there is $u_{\text{ini}}=0$.

Eqs. (7) and (8) were adopted for the FE analysis. The domain was discretized using three-noded triangular elements. The discretized versions of Eqs. (7) and (8) were solved following an implicit (backward difference) numerical time integration scheme. A detailed description of the FE derivation is given in Basu et al. (2005).

The FE solution was obtained by writing a FORTRAN program. In order to check convergence, the element size was varied until two successive meshes produced identical results (difference less than 0.01%). For the final accepted mesh, the length of the elements adjacent to the PVD was 25 mm, increasing gradually to up to a maximum of 110 mm at the cell boundaries. The time step ΔT was taken equal to $0.001T$ for $T \leqslant 0.1$ and equal to $0.01T$ for $T > 0.1$.

The accuracy of the FE analysis was checked against the analytical solutions of Barron (1948) and Hansbo (1981). According to Barron (1948), the degree of consolidation U for "equal-strain" consolidation is given by

$$U = 1 - \exp\left(-\frac{8T}{\mu}\right) \tag{9}$$

with

$$\mu = \left(\frac{n^2}{n^2-1}\right)\ln n - \frac{3n^2-1}{4n^2} \tag{10}$$

and

$$n = \frac{d_c}{d_w} \tag{11}$$

where d_c and d_w=circular unit cell and drain diameters, respectively. Hansbo (1981) introduced a circular smear zone (of diameter d_s) in the solution which resulted in a modified expression for μ

$$\mu = \ln\left(\frac{n}{m}\right) + \frac{k_{ho}}{k_{hs}} \ln m - \frac{3}{4} \tag{12}$$

with

$$m = \frac{d_s}{d_w} \tag{13}$$

For comparison purposes, the area of the unit cell was converted to an equivalent circle of diameter $d_{c,\text{eq}}$ [Eq. (5)], which was then used in the analytical solution as the diameter d_c. The equivalent diameter $d_{w,\text{eq}}$ of the band-shaped PVD is obtained by equating the perimeter of the PVD to that of a circle (Hansbo 1981)

$$d_{w,\text{eq}} = \frac{2}{\pi}(d_b + d_t) \tag{14}$$

where d_b and d_t=PVD width and thickness, respectively. $d_{w,\text{eq}}$ is taken equal to the diameter d_w of the circular drain of the analytical case. For a 100 mm×4 mm PVD, $d_{w,\text{eq}}=66.2$ mm. The rectangular smear zone of dimensions $l_x \times l_y$ is converted to an equivalent circle with a diameter $d_{s,\text{eq}}$ given by

$$d_{s,\text{eq}} = \sqrt{\frac{4 l_x l_y}{\pi}} \tag{15}$$

$d_{s,\text{eq}}$ is used as the diameter d_s of the circular smear zone in the analytical solution.

Comparisons were made for the cases with and without smear for a spacing $s=1$ m and a mandrel of 125×50 mm. The smear zone was assumed to extend to $2d$, where d is the smaller dimension of the mandrel cross section. A value of 0.2 was assumed for the k_{hs}/k_{ho} ratio. The results of the FE analyses were found to compare well with the analytical solutions (Basu et al. 2005). The maximum difference in U, for $U > 50\%$, was about 3.3%, occurring at $T=0.3$ for the case without smear zone, and, for the case with smear zone, the maximum difference in U was 5%, occurring at $T=0.7$.

Results

Effect of Soil Disturbance

In design, it is very important to account for the detrimental effects of soil disturbance on PVD-enhanced consolidation. The effects of the smear and transition zones on the degree of consolidation are investigated for two cases: (1) PVD installed with a mandrel of 125×50 mm at 1-m spacing (Combination 1), and (2) PVD installed with a mandrel of 150×150 mm at 3-m spacing (Combination 2). The degree of disturbance, quantified in terms of k_{hs}/k_{ho}, is maintained constant at a value of 0.2. The smear and transition zones are assumed to extend to $2d$ ($p=2$) and $12d$ ($p=12$), respectively. Fig. 3 shows the U versus T curves for Combination 1. It is clear that soil disturbance has a substantial detrimental effect on the effectiveness of PVDs in accelerating consolidation. For Combination 1 (Fig. 3), T required for 90% consolidation is equal to 0.65, 1.76, and 2.35 for the following three conditions: (1) absence of a smear zone; (2) presence of a smear zone only; and (3) presence of both smear and transition zones. Compared to the no-disturbance condition, T (for $U=90\%$) increases by 171% if only the smear zone is considered, and by 262%, if both the smear and transition zones are considered. The difference in T between the cases with only the smear zone and both the smear and transition zones is 34%. For Combination 2 (not plotted), T corresponding to 90% consolidation is equal to 0.95 in the absence of a smear zone, 2.98 in the presence of a smear zone only, and 3.72 in the presence of both smear and transition zones. Again, compared with the no-disturbance condition, the increase in T considering the existence of a smear zone only is 214%; if both the smear and transition zones are considered, T increases by 292%. The increase in T for the case where both a smear and a transition zone are present over the case where only a smear zone is present is 25%.

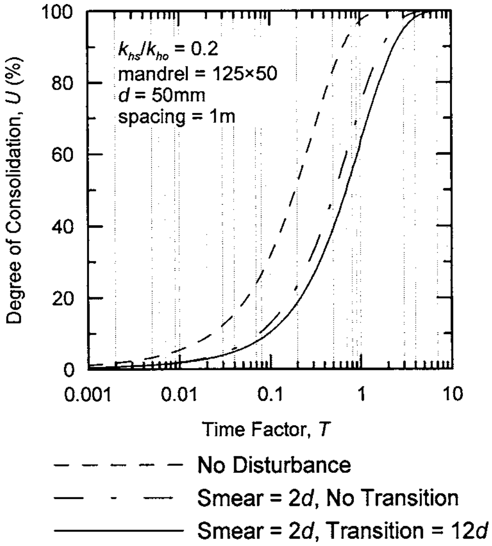

Fig. 3. Effect of soil disturbance on consolidation rate

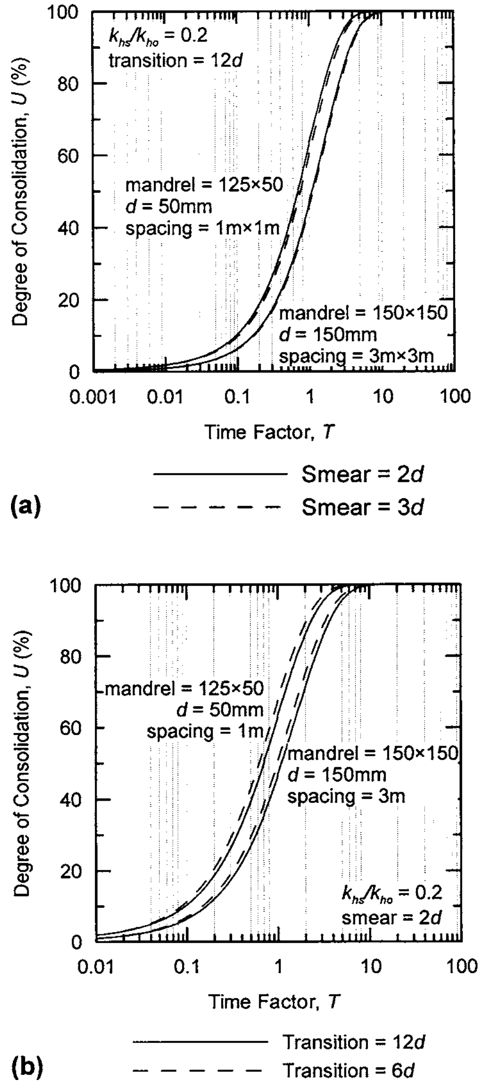

Fig. 4. Effect of disturbed zone dimension on consolidation rate: (a) effect of smear zone dimension; (b) effect of transition zone dimension

Disturbed Zone Dimensions

In order to evaluate the extent to which the dimensions of the smear zone affect PVD performance, two dimensions of the smear zone, corresponding to l_y equal to $2d$ and $3d$, are compared for a fixed transition zone size t_y equal to $12d$. The same Combinations 1 and 2 described earlier with $k_{hs}/k_{ho}=0.2$ are considered [Fig. 4(a)]. For Combination 1, T required for 90% consolidation is equal to 2.35 and 2.55 for a smear zone size l_y equal to $2d$ and $3d$, respectively; the difference between the two cases being 8.5%. For Combination 2, T required for 90% consolidation is equal to 3.73 and 3.89 for l_y equal to $2d$ and $3d$, respectively; the difference between the two cases being 4.3%. Thus, the extent of the smear zone has a moderate impact on the rate of consolidation.

As the size t_y of the transition zone is likely to be in the $6d$ to $12d$ range, it is necessary to investigate how the consolidation rate varies for transition zone sizes in this range. Therefore, values of t_y equal to $6d$ and $12d$, with a fixed smear zone size l_y equal to $2d$, were used in the analysis. As before, the same two combinations, with $k_{hs}/k_{ho}=0.2$, are studied [Fig. 4(b)]. For Combination 1, T values corresponding to 90% consolidation are equal to 2.07 and 2.35 for t_y equal to $6d$ and $12d$, respectively; the difference being 13.5%. For Combination 2, T values corresponding to $U=90\%$ are equal to 3.34 and 3.73 for t_y equal to $6d$ and $12d$, respectively, corresponding to a difference of 11.7%. Thus, the larger the smear and transition zone dimensions, the slower the consolidation rate is.

Degree of Disturbance

The degree of soil disturbance is accounted for by the ratio k_{hs}/k_{ho}. Fig. 5 shows the U versus T curves for k_{hs}/k_{ho} ranging from 0.05 to 0.5 and PVDs installed with a mandrel of 125×50 mm at 1-m spacing. The smear and the transition zone dimensions l_y and t_y are taken as $2d$ and $12d$, respectively. The values of T corresponding to $U=90\%$ are 7.36, 4.13, 2.35, 1.69, and 1.11 for k_{hs}/k_{ho} equal to 0.05, 0.1, 0.2, 0.3, and 0.5, respectively. For PVDs installed with a mandrel of 150×150 mm at 3-m spacing (not plotted), the corresponding values of T are 12.43, 6.76, 3.73, 2.62, and 1.7. Interestingly, the variation of T with k_{hs}/k_{ho}, for a constant U, follows a power law (Fig. 6). Therefore, for a given value of U, T can be expressed in terms of k_{hs}/k_{ho} as

$$T=C_1\left(\frac{k_{hs}}{k_{ho}}\right)^{-C_2} \tag{16}$$

where C_1 and C_2=real positive numbers.

Clearly, the degree of disturbance has a significant effect on the consolidation rate. The impact of the degree of disturbance on the consolidation rate is much more pronounced than that of the dimensions of the smear and transition zones. Therefore, the degree of disturbance needs to be predicted with greater accuracy than the extent of the zones of disturbance surrounding the PVD in order to produce an optimal design.

PVD Spacing

The rate of consolidation decreases with increasing PVD spacing. In order to evaluate the benefit of reducing the PVD spacing, three different spacings (1, 2, and 3 m) are considered for the 125×50 mm mandrel (Fig. 7). The smear and the transition zone

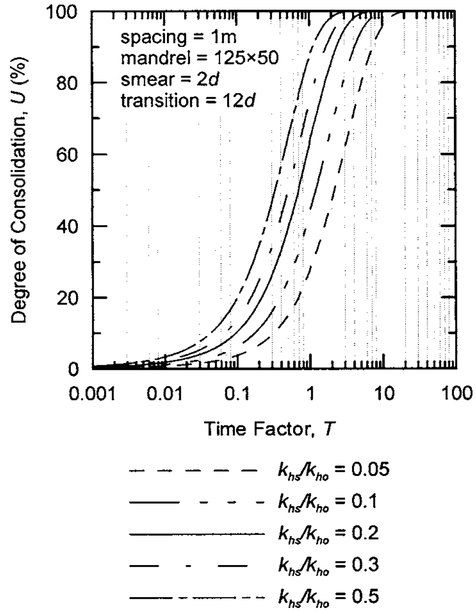

Fig. 5. Effect of degree of disturbance on consolidation rate

dimensions l_y and t_y are fixed at $2d$ and $12d$, respectively, with $k_{hs}/k_{ho}=0.2$. It is found that consolidation occurs at a faster rate for smaller PVD spacing. For $U=90\%$, T decreases by 4.4% when the spacing is reduced from 3 to 2 m, and by 9%, when it is reduced further from 2 to 1 m.

Also plotted in Fig. 7 are the U versus T curves for the corresponding cases where no soil disturbance is considered. Here, a decrease in T of 12.6% (corresponding to $U=90\%$) occurs when the PVD spacing is reduced from 3 to 2 m; a reduction of 21.7% in T occurs when the spacing is decreased from 2 to 1 m.

If no soil disturbance is considered in the calculations, then the estimated increase in the consolidation rate obtained by reducing the PVD spacing is substantially larger than the actual increase that takes place in the presence of the soil disturbance caused by PVD installation.

Mandrel Size and Shape

The effect of mandrel size is studied for two different PVD spacings (1 and 3 m), with smear and transition zone dimensions l_y and t_y equal to $2d$ and $12d$, respectively, and a ratio k_{hs}/k_{ho} of 0.2. Four different mandrel sizes: 125×50, 150×50, 120×120 and 150×150 mm are used in the study. Fig. 8 shows the U versus T curves for the 1-m PVD spacing. The values of T, corresponding to $U=90\%$, are 2.35, 2.4, 3.22, and 3.23 for the four mandrel sizes mentioned earlier (in the same order). For 3-m spacing (not plotted), the corresponding values of T are 2.7, 2.75, 3.5, and 3.73, respectively.

The rate of consolidation decreases with increasing mandrel sizes, although, for practical purposes, the 150×50 mm mandrel is as effective as the 125×50 mm mandrel. The same can be stated about the 120×120 and 150×150 mm mandrels. However, there is a substantial difference in the consolidation rate when rectangular mandrels and square mandrels are compared. Square mandrels are less effective than rectangular mandrels be-

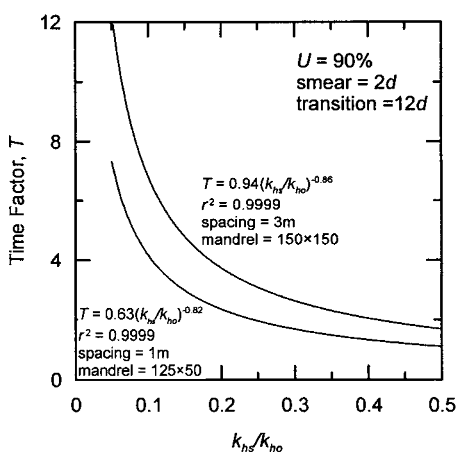

Fig. 6. Dependence of time factor on the degree of disturbance

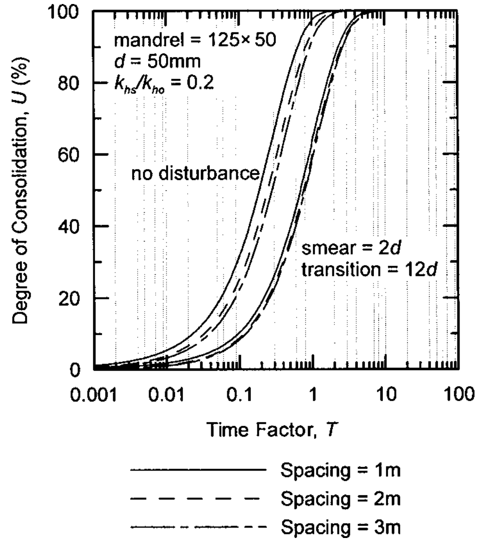

Fig. 7. Effect of PVD spacing on consolidation rate

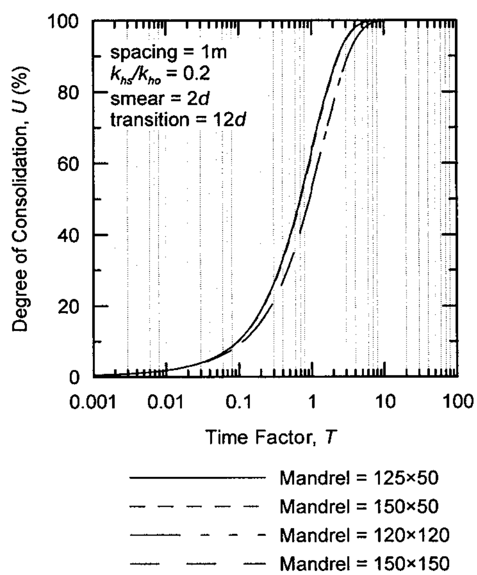

Fig. 8. Effect of mandrel size on consolidation rate (the curves for the 125×25 mm mandrel and the 125×50 mm mandrel almost coincide; this is also the case for the curves of the 120×120 mm mandrel and the 150×150 mm mandrel)

Table 1. Replacement of the Transition Zone by an Expanded Smear Zone

k_{hs}/k_{ho}	Extra length of smear zone per unit length of transition zone
0.1	0.13
0.2	0.20
0.3	0.25

cause they disturb a much larger area. This finding is in agreement with the results of a laboratory study by Hird and Sangtian (2002), which indicates that the smear effect is reduced by replacing circular mandrels with slim rectangular mandrels.

Lessons for Design

Replacement of Transition Zone by an Equivalent Smear Zone

A way of accounting for the transition zone in design is to replace the transition zone and the smear zone with a single equivalent smear zone. In this paper, the extra length of smear zone required to replace the transition zone was determined by studying several combinations of spacings (1, 2, and 3 m) and mandrels (125×50, 150×50, 120×120, and 150×150 mm) for two different smear zone dimensions ($l_y=2d$ and $3d$), three different transition zone dimensions ($t_y=6d$, $9d$, and $12d$), and three different values of k_{hs}/k_{ho} (0.1, 0.2, and 0.3).

It was found that the extra length of the smear zone required to replace the transition zone depends only on the k_{hs}/k_{ho} ratio and the size of the transition zone itself, as shown in Table 1. For example, if the original domain consists of a smear zone with $l_y=3d$ and a transition zone with $t_y=9d$, then $6d$ is the length of the transition zone that needs to be replaced. Assuming a k_{hs}/k_{ho} of 0.3 and referring to Table 1, the extra length of smear zone required is $0.25\times6d=1.5d$. Therefore the equivalent smear zone extends to $3d+1.5d=4.5d$. As can be seen in Fig. 9, which shows the U versus T curves obtained for the original domain considering both smear and transition zones and the equivalent domain

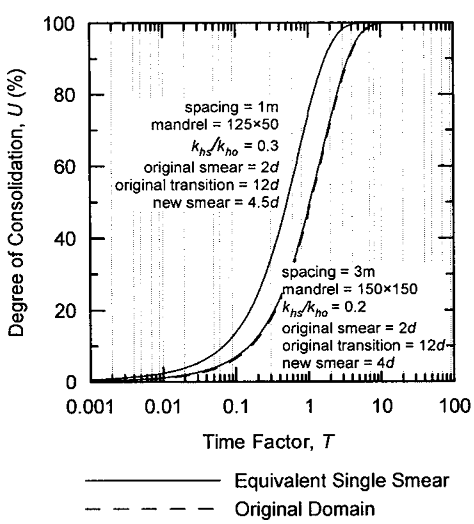

Fig. 9. Replacement of original domain with smear and transition zones by an equivalent domain with an expanded smear zone

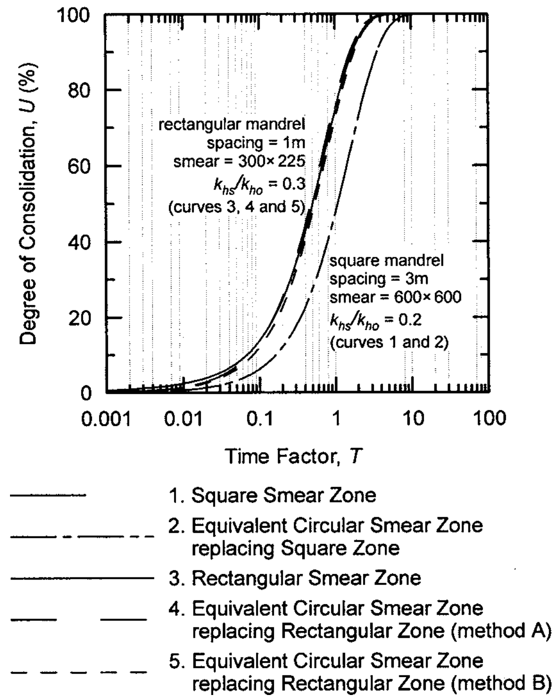

Fig. 10. U versus T curves for square, rectangular, and equivalent circular smear zones (Curves 1 and 2 are almost coincident; Curves 3–5 are very close to each other, with Curve 3 lying to the right of Curve 4 and to the left of Curve 5 for $T>0.5$)

with a smear zone only, this procedure works quite well for all the cases considered. However, it is not applicable when there is overlap of adjacent transition zones.

Equivalent Circular Smear Zone

The procedure outlined in the previous section facilitates the design process to a great extent as a single equivalent smear zone is used in design. Nonetheless, the rectangular smear zone still needs to be converted to an equivalent circle to allow use of the available analytical solutions (Hansbo 1981). Two methods (A and B) can be used to do this conversion. In Method A, two steps need to be followed:

(1) Estimate the dimensions of the rectangular smear zone ($l_x\times l_y$) from the mandrel dimensions ($a\times d$) by using Eqs. (1) and (2).
(2) Convert the rectangular area of the smear zone into an equivalent circle; Eq. (15), which gives the equivalent diameter $d_{s,\mathrm{eq}}$ of the circle, is used for this purpose.

Alternatively, in Method B, the procedure is as follows:

(1) Convert the rectangular mandrel with dimensions $a\times d$ to an equivalent circle by using Eq. (15) (with l_x and l_y replaced by a and d, respectively) to obtain the equivalent mandrel diameter $d_{m,\mathrm{eq}}$.
(2) Multiply $d_{m,\mathrm{eq}}$ by the constant p of Eqs. (1) and (2) to obtain the equivalent smear zone diameter $d_{s,\mathrm{eq}}$.

For square mandrels, both methods yield the same smear zone diameter. Several combinations of spacings, square mandrel sizes, smear and transition zone dimensions, and degrees of disturbance were studied. The difference between values of U obtained considering square smear zones and the corresponding equivalent circles was negligible. Fig. 10 shows the results for 3-m spacing with a square smear zone of dimensions 600×600 mm and

$k_{hs}/k_{ho}=0.2$. For this particular case, the maximum difference in the resulting U value for the square and equivalent circular smear zones is less than 1%. This illustrates that for square-shaped smear zones, the error in converting the square disturbance zone to equivalent circle is negligible.

For rectangular mandrels, the maximum difference in U values obtained for rectangular smear zones and the corresponding equivalent circles is about 5%. In all cases, the U versus T curves obtained for a rectangular smear zone always lie between the curves obtained for the corresponding equivalent circular smear zones (with the diameter $d_{s,\mathrm{eq}}$ obtained by Methods A and B). Method B is recommended for use in design as it always produced conservative results (for large time factors). Fig. 10 shows the U versus T curves for a mandrel size of 125×50 mm and PVD spacing of 1 m [with p of Eqs. (1) and (2) taken as 4.5]. The ratio k_{hs}/k_{ho} is taken as equal to 0.3.

Time Factor

In order to facilitate the design procedure further, the constants C_1 and C_2 of Eq. (16) are obtained for $U=50\%$ and $U=90\%$ and $s=1$, 2, and 3 m. Equivalent circular unit cells with equivalent circular smear zones are assumed. These constants are given in Table 2 for different ratios of equivalent circular smear zone diameter to equivalent circular unit cell diameter. For the mandrels considered in this paper, it was found that the equivalent diameter of the expanded smear zone $d_{s,\mathrm{eq}}$ can range anywhere from 0.15 to 1.0 times the equivalent diameter of the unit cell $d_{c,\mathrm{eq}}$. Hence, the values of C_1 and C_2 are obtained for $d_{s,\mathrm{eq}}/d_{c,\mathrm{eq}}=0.1-1.0$; in intervals of 0.1. Using these values, a designer can directly determine T required for 50% or 90% consolidation for a given PVD spacing, equivalent smear zone dimension, and degree of disturbance.

Numerical Example

A practical example problem is worked out in this section to facilitate the understanding of the method proposed in this paper. A site with $c_h=2$ m^2/year is considered, where a 125×50 mm mandrel is to be used for installation of PVDs in a triangular pattern. The PVD cross-section dimensions are 100 mm$\times$4 mm ($d_{w,\mathrm{eq}}=66.2$ mm). The degree of disturbance given by k_{hs}/k_{ho} is assumed to be equal to 0.2. The smear and transition zone dimensions l_y and t_y are assumed to be equal to $2d$ and $12d$, respectively. Thus, a transition zone of length $12d-2d=10d$ is to be replaced by an extra length of smear zone. Using Table 1, for $k_{hs}/k_{ho}=0.2$, the additional length of smear zone required is $0.2\times10d=2d$. Therefore, the equivalent smear zone extends to $4d$ ($2d+2d$). For estimating the equivalent circular smear zone diameter, Method B, as described in the previous section, is used. The diameter $d_{m,\mathrm{eq}}$ of the equivalent circular mandrel is 89.2 mm [Eq. (15)]. This means that the diameter $d_{s,\mathrm{eq}}$ of the equivalent smear zone is $4\times89.2=356.8$ mm and $m=5.39$ [Eq. (13)]. For a PVD spacing of 1 m, the diameter $d_{c,\mathrm{eq}}$ of the equivalent circular unit cell is 1.05 m [Eq. (5)], which results in $n=15.86$ [Eq. (11)]. This yields $\mu=8.75$ [Eq. (12)]. Assuming that 90% consolidation is to be achieved, T required is 2.52 [Eq. (9)]. Alternatively, T (for $U=90\%$) can be obtained from Table 2. For $k_{hs}/k_{ho}=0.2$, $s=1$ m (i.e., $d_{c,\mathrm{eq}}=1.05$ m) and $d_{s,\mathrm{eq}}/d_{c,\mathrm{eq}}=0.34$, values of C_1 and C_2 are obtained by linear interpolation between $d_{s,\mathrm{eq}}/d_{c,\mathrm{eq}}=0.3$ and 0.4 ($C_1=0.5383$ and $C_2=0.9611$). This yields $T=0.5383(0.2)^{-0.9611}=2.53$ [Eq. (16)], which corresponds to a time equal to 1.4 years ($c_h=2$ m^2/year and $d_{c,\mathrm{eq}}=1.05$ m; [Eq. (4)]).

Table 2. Values of the Constants C_1 and C_2 of Eq. (16) for $U=50\%$ and $U=90\%$ and Various Values of PVD Spacing and $d_{s,\mathrm{eq}}/d_{c,\mathrm{eq}}$

Spacing (m)	$d_{s,\mathrm{eq}}/d_{c,\mathrm{eq}}$ [a]	C_1 $U=50\%$	C_1 $U=90\%$	C_2
1	0.1	0.1290	0.4287	0.6294
	0.2	0.1442	0.4790	0.8765
	0.3	0.1579	0.5244	0.9467
	0.4	0.1683	0.5591	0.9827
	0.5	0.1766	0.5867	1.0054
	0.6	0.1835	0.6097	1.0215
	0.7	0.1895	0.6294	1.0335
	0.8	0.1946	0.6465	1.0431
	0.9	0.1992	0.6617	1.0509
	1.0	0.2033	0.6754	1.0574
2	0.1	0.1823	0.6056	0.8009
	0.2	0.2035	0.6761	0.9181
	0.3	0.2178	0.7235	0.9623
	0.4	0.2283	0.7585	0.9873
	0.5	0.2367	0.7862	1.0041
	0.6	0.2436	0.8092	1.0163
	0.7	0.2495	0.8287	1.0258
	0.8	0.2546	0.8457	1.0334
	0.9	0.2591	0.8609	1.0398
	1.0	0.2632	0.8744	1.0452
3	0.1	0.2160	0.7176	0.8429
	0.2	0.2385	0.7921	0.9316
	0.3	0.2529	0.8401	0.9678
	0.4	0.2635	0.8752	0.9891
	0.5	0.2718	0.9029	1.0035
	0.6	0.2787	0.9258	1.0143
	0.7	0.2846	0.9453	1.0227
	0.8	0.2897	0.9623	1.0296
	0.9	0.2942	0.9774	1.0353
	1.0	0.2983	0.9909	1.0402

[a]Ratio of the equivalent smear zone diameter to the equivalent unit cell diameter.

In order to investigate how much the PVD spacing affects the rate of consolidation in the presence of soil disturbance, the same example is solved for different PVD spacings, as shown in Table 3. It is found that, although the values of the time factor T corresponding to $U=90\%$ for spacings of, say, 3 and 1 m do not differ much, the actual times do differ substantially because time depends not only on T but also on the square of the equivalent cell diameter. Thus, there is a significant benefit from installing PVDs at closer spacing if time is of the essence.

Conclusions

The paper examined the effect of soil disturbance on the rate of consolidation of a soil deposit engineered with PVDs. A standard PVD cross section of 100 mm$\times$4 mm and a triangular PVD installation pattern were considered throughout. The analysis was performed using finite elements following the Terzaghi-Rendulic theory of consolidation. PVD installation creates two distinct zones of disturbance: (1) a completely remolded smear zone and (2) a less disturbed transition zone. The hydraulic conductivity was assumed to increase linearly in the transition zone from a low

Table 3. Example Showing the Effect of PVD Spacing

Spacing (m)	$d_{c,\mathrm{eq}}$ (mm)	$d_{w,\mathrm{eq}}$ (mm)	$d_{s,\mathrm{eq}}$ (mm)	n	m	k_{hs}/k_{ho}	T	t (years)
0.9	945.1	66.2	356.8	14.28	5.39	0.2	2.49	1.1
1.0	1,050.1	66.2	356.8	15.86	5.39	0.2	2.52	1.4
1.5	1,575.1	66.2	356.8	23.79	5.39	0.2	2.64	3.3
2.0	2,100.2	66.2	356.8	31.73	5.39	0.2	2.72	6.0
3.0	3,150.2	66.2	356.8	47.59	5.39	0.2	2.84	14.1

value in the smear zone to the original in situ value in the undisturbed zone. The actual hexagonal shape of the unit cell, band shape of the drain, and rectangular shape of the smear and transition zones were used in the analysis.

It was observed that soil disturbance reduces significantly the PVD consolidation rate, and the transition zone has a definite impact on the consolidation process. Larger smear and transition zones result in slower consolidation rates. However, it is the degree of disturbance, quantified by the decrease in the hydraulic conductivity, that affects the process the most. PVD spacing and mandrel size and shape also influence PVD performance. A method of replacing the transition zone by an equivalent expanded smear zone is proposed so that the existing (simple) analytical solutions can be used. Additionally, a method of converting the rectangular smear zone to an equivalent circle is proposed that always produces safe design.

Acknowledgments

The writers acknowledge the financial support received from Fugro N.V., provided in the form of a Fugro Fellowship, and are very grateful to Fugro, Nick Aschliman, and Joe Cibor for this support.

References

Akagi, T. (1994). "Hydraulic applications of geosynthetics to some filtration and drainage problems with special reference to prefabricated band-shaped drains." *Proc., 5th Int. Conf. on Geotextiles Geomembranes Related Products*, Singapore, 1339–1359.

American Wick Drain Corporation. (2004). "Installing AMERDRAIN® vertical drain." ⟨http://www.americanwick.com/vdinstall.shtml⟩ (Sep. 7, 2005).

Barron, R. A. (1948). "Consolidation of fine-grained soils by drain wells." *Trans. ASCE*, 113, 718–742, (reprinted in *A history of progress*, ASCE, Reston, Va., 2003, Vol. 1, 324–348).

Basu, D., Basu, P., and Prezzi, M. (2005). "Study of consolidation by prefabricated vertical drain." *Internal Geotechnical Rep. No. 2005-01*, Purdue Univ., West Lafayette, Ind.

Basu, D., and Madhav, M. R. (2000). "Effect of prefabricated vertical drain clogging on the rate of consolidation: A numerical study." *Geosynthet. Int.*, 7(3), 189–215.

Bergado, D. T., Alfaro, M. C., and Balasubramaniam, A. S. (1993a). "Improvement of soft Bangkok clay using vertical drains." *Geotext. Geomembr.*, 12(7), 615–663.

Bergado, D. T., Anderson, L. R., Miura, N., and Balasubramaniam, A. S. (1996). "Prefabricated vertical drains (PVD)." *Soft ground improvement in lowland and other environments*, ASCE, Reston, Va., Chap. 4, 88–185.

Bergado, D. T., Asakami, H., Alfaro, M. C., and Balasubramaniam, A. S. (1991). "Smear effects on vertical drains on soft Bangkok clay." *J. Geotech. Engrg.*, 117(10), 1509–1530.

Bergado, D. T., Mukherjee, K., Alfaro, M. C., and Balasubramaniam, A. S. (1993b). "Prediction of vertical-band-drain performance by the finite-element method." *Geotext. Geomembr.*, 12(6), 567–586.

Casagrande, L., and Poulos, S. (1969). "On the effectiveness of sand drains." *Can. Geotech. J.*, 6(3), 287–326.

Chai, J.-C., and Miura, N. (1999). "Investigation of factors affecting vertical drain behavior." *J. Geotech. Geoenviron. Eng.*, 125(3), 216–226.

Chai, J. C., Miura, N., and Sakajo, S. (1997). "A theoretical study on smear effect around vertical drain." *Proc., 14th Int. Conf. on Soil Mechanics and Foundations Engineering*, Hamburg, Germany, 1581–1584.

Cook, R. D., Malkus, D. S., Plesha, M. E., and Witt, R. J. (2002). *Concepts and applications of finite element analysis*, 4th Ed., Wiley, New York.

Hansbo, S. (1981). "Consolidation of fine-grained soils by prefabricated drains." *Proc., 10th Int. Conf. on Soil Mechanics and Foundations Engineering*, Stockholm, Sweden, Vol. 3, 677–682.

Hansbo, S. (1986). "Preconsolidation of soft compressible subsoil by the use of prefabricated vertical drains." *Annales des Travaux Publics de Belgique*, No. 6, 553–563.

Hansbo, S. (1987). "Design aspects of vertical drains and lime column installations." *Proc., 9th Southeast Asian Geotech. Conf.*, Bangkok, Thailand, 1–12.

Hansbo, S. (1997). "Practical aspects of vertical drain design." *Proc., 14th Int. Conf. on Soil Mechanics and Foundations Engineering*, Hamburg, Germany, Vol. 3, 1749–1752.

Hawlader, B. C., Imai, G., and Muhunthan, B. (2002). "Numerical study of the factors affecting the consolidation of clay with vertical drains." *Geotext. Geomembr.*, 20(4), 213–239.

Hird, C. C., and Moseley, V. J. (2000). "Model study of seepage in smear zones around vertical drains in layered soil." *Geotechnique*, 50(1), 89–97.

Hird, C. C., and Sangtian, N. (2002). "Model study of seepage in smear zones around vertical drains in layered soil: Further results." *Geotechnique*, 52(5), 375–378.

Holtz, R. D. (1987). "Preloading with prefabricated vertical strip drains." *Geotext. Geomembr.*, 6(1–3), 109–131.

Holtz, R. D., and Holm, B. G. (1973). "Excavation and sampling around some sand drains in Skå-Edeby, Sweden." *Sartryck och Preliminara Rapporter*, Issue 51, 79–85.

Holtz, R. D., Jamiolkowski, M. B., Lancellotta, R., and Pedroni, R. (1991). *Prefabricated vertical drains: Design and performance*, Butterworth-Heinemann, Oxford, U.K.

Indraratna, B., and Redana, I. W. (1997). "Plane-strain modeling of smear effects associated with vertical drains." *J. Geotech. Geoenviron. Eng.*, 123(5), 474–478.

Indraratna, B., and Redana, I. W. (1998). "Laboratory determination of smear zone due to vertical drain installation." *J. Geotech. Geoenviron. Eng.*, 124(2), 180–184.

Jamiolkowski, M., Lancellotta, R., and Wolski, W. (1983). "Precompression and speeding up consolidation." *Improvement of ground: Proc., 8th European Conf. on Soil Mechanics and Foundations Engineering*, Balkema, Rotterdam, The Netherlands, Vol. 3, 1201–1226.

Leo, C. J. (2004). "Equal strain consolidation by vertical drains." *J. Geotech. Geoenviron. Eng.*, 130(3), 316–327.

Madhav, M. R., Park, Y.-M., and Miura, N. (1993). "Modelling and study of smear zones around band shaped drains." *Soils Found.*, 33(4), 135–147.

Mesri, G., Lo, D. O. K., and Feng, T.-W. (1994). “Settlement of embankments on soft clays.” *Geotech. Spec. Publ.*, No. 40, 8–56.

Miura, N., Park, Y., and Madhav, M. R. (1993). “Fundamental study on drainage performance of plastic-board drains.” *J. Geotech. Engrg.*, 481/III-25, No. 12, 31–40.

Onoue, A., Ting, N.-H., Germaine, J. T., and Whitman, R. V. (1991). “Permeability of disturbed zone around vertical drains.” *Geotech. Spec. Publ.*, No. 27, 879–890.

Rendulic, L. (1935). “Der hydrodynamische spannungsausgleich in zentral entwässerten Tonzylindern.” *Wasserwirtschaft und Technik*, 2, No. 23–26, 250–253.

Rendulic, L. (1936). “Porenziffer und porenwasserdruck in Tonen.” *Bauingenieur*, 17, December, 559–564.

Saye, S. R. (2003). “Assessment of soil disturbance by the installation of displacement sand drains and prefabricated vertical drains.” *Geotech. Spec. Publ.*, No. 119, 325–362.

Sharma, J. S., and Xiao, D. (2000). “Characterization of a smear zone around vertical drains by large-scale laboratory tests.” *Can. Geotech. J.*, 37(6), 1265–1271.

Terzaghi, K. (1925). *Erdbaumechanik auf bodenphysikalischer grundlage*, Deuticke, Vienna, Austria (in German).